ROME prep. 973/93
INFN-ISS 93/6
ULB-TH 15/93
November 1993

Leading Order QCD Corrections to $b \to s\,\gamma$ and $b \to s\,g$ Decays in Three Regularization Schemes

M. Ciuchini[a,b], E. Franco[b], L. Reina[c] and L. Silvestrini[b]

[a] INFN, Sezione Sanità, V.le Regina Elena 299, 00161 Roma, Italy.
[b] Dip. di Fisica, Università degli Studi di Roma "La Sapienza" and INFN, Sezione di Roma, P.le A. Moro 2, 00185 Roma, Italy.
[c] Service de Physique Théorique[1], Université Libre de Bruxelles, Boulevard du Triomphe, CP 225 B-1050 Brussels, Belgium.

Abstract

We discuss in detail the calculation of the leading order QCD corrections to the Effective Hamiltonian which governs $b \to s\,\gamma$ and $b \to s\,g$ transitions in three different regularization schemes (HV, NDR and DRED). We show that intermediate stages of the calculation do depend on the regularization, but the same scheme independent coefficients can be obtained in all the considered schemes. A detailed discussion of the results already present in the literature is also given.

[1] Chercheur IISN

1 Introduction

Leading order (LO) QCD corrections to the Effective Hamiltonian governing the radiative decays of the B meson have been calculated by many authors in the last five years [1]-[7]. In fact they turn out to be large and important for the B phenomenology. In spite of this effort, different results are still present in the recent literature on this subject, even if the residual differences are numerically small and have essentially no phenomenological relevance. The aim of this paper is to help clarifying the origin of these differences by giving full details on our calculations in three different regularization schemes.

Let us briefly recall how the calculation of LO corrections to the Effective Hamiltonian for radiative B decays has been developed in the recent years. The original calculations, refs. [1] and [2], were performed in the Naive Dimensional Regularization scheme (NDR) and in the Dimensional REDuction scheme (DRED [8]) respectively and used a reduced set of operators for the Effective Hamiltonian. They disagree on the results for the anomalous dimension matrix, that was believed to be regularization scheme independent at the leading order.

Later NDR result was confirmed [3] and this led the authors of ref. [9] to cast doubts on the reliability of the DRED scheme. Two years ago a first paper [4] appeared where the complete LO correction was calculated in the NDR scheme using the full set of operators, then other similar calculations followed [5]-[6]. Refs. [5] and [6] confirm the result of ref. [1] for the anomalous dimension matrix in the "reduced" basis. However they disagree on some new matrix elements in the "full" basis.

Recently the question of the scheme independence of the Effective Hamiltonian for B meson radiative decays has been clarified [7]. The calculation of the complete LO corrections has been performed in NDR and in the 't Hooft-Veltman scheme (HV [10]) and it has been shown that the final results for the Wilson coefficients are regularization scheme independent provided one takes properly into account the scheme dependence of the one and two loop Feynman diagrams. Calculations which use the reduced set of operators such as those of refs. [1, 2, 3] have been demonstrated to give results which depend on the regularization scheme. Unfortunately the new NDR anomalous dimension matrix obtained in ref. [7] differs from both the results of refs. [5, 6].

In this paper we provide full details on the calculation presented in ref. [7], including tables with the pole coefficients for all the diagrams. We also present the calculation in the DRED scheme. We show how the same regularization independent results can be obtained in DRED as well as in the other two schemes, thus extending the result of ref. [11]. We also discuss why the conclusions of ref. [9] on the reliability of the DRED scheme are wrong. Finally we compare our results with the most recent ones [5, 6] and comment on the differences among the results, reported in refs. [11, 12].

The paper is organized as follows. In Sec. 2 we recall the Effective Hamiltonian for $b \to s\,\gamma$ decays and the renormalization group equations (RGE) governing the evolution of the Wilson coefficients. The full operator basis is given and compared with the reduced one. The initial conditions for the coefficients are also given. In Sec. 3 the explicit solution of the RGE, showing the scheme independence of the coefficients, is given. In Sec. 4 we summarize the definitions of NDR, HV and DRED regularization schemes, discussing how they are implemented in our calculations. In Sec. 5 the contributions of one loop diagrams to anomalous dimension, operator matrix elements and counter-terms are considered and diagram by diagram results are given. The same is done for the contributions of the two loop diagrams to the anomalous dimension. We discuss the relations among one and two loop diagrams induced by the scheme independence of the final result and briefly report other checks done on our calculation. In Sec. 6 the anomalous dimension matrices in the different schemes are given. Finally in Sec. 7 we critically compare our results with the other ones present in the literature.

2 Effective Hamiltonian: Initial Conditions and Evolution for the Coefficients

The effective Hamiltonian for $b \to s\,\gamma$ ($b \to s\,g$) transitions is given by

$$H_{eff} = -V_{tb}V_{ts}^{*}\frac{G_F}{\sqrt{2}}\sum_{i=1}^{8} Q_i(\mu)C_i(\mu) \sim \vec{Q}^T(\mu)\,\vec{C}(\mu) \tag{1}$$

where V_{ij} are the elements of the CKM[13, 14] quark mixing matrix. We use the following operator basis $\vec{Q}$

$$
\begin{aligned}
Q_1 &= (\bar{s}_\alpha c_\beta)_{(V-A)}(\bar{c}_\beta b_\alpha)_{(V-A)} \\
Q_2 &= (\bar{s}_\alpha c_\alpha)_{(V-A)}(\bar{c}_\beta b_\beta)_{(V-A)} \\
Q_{3,5} &= (\bar{s}_\alpha b_\alpha)_{(V-A)} \sum_{q=u,d,s,\cdots} (\bar{q}_\beta q_\beta)_{(V\mp A)} \\
Q_{4,6} &= (\bar{s}_\alpha b_\beta)_{(V-A)} \sum_{q=u,d,s,\cdots} (\bar{q}_\beta q_\alpha)_{(V\mp A)} \\
Q_7 &= \frac{Q_d e}{16\pi^2} m_b \bar{s}_\alpha \sigma^{\mu\nu}_{(V+A)} b_\alpha F_{\mu\nu} \\
Q_8 &= \frac{g}{16\pi^2} m_b \bar{s}_\alpha \sigma^{\mu\nu}_{(V+A)} t^A_{\alpha\beta} b_\beta G^A_{\mu\nu}.
\end{aligned} \tag{2}
$$

Here $(V \mp A)$ indicate the chiral structure, α and β are colour indices, m_b is the b quark mass, $Q_d = -\frac{1}{3}$ is the electric charge of the down-type quarks and g (e) is the strong (electro-magnetic) coupling. The colour matrices normalization is $Tr(t^A t^B) = \delta^{AB}/2$.

The choice of the operator basis deserves some comments. In fact the basis in eq. (2) is obtained by using the equations of motion of the external fields. While this procedure has been criticized in the past, a recent paper [16] shows that it can be safely used. This basis is often called the "complete" basis, to be compared with the "reduced" one of refs. [1, 2, 3]. Using the "reduced" basis, one neglects the contributions of the operators $Q_3, \ldots, Q_6$. Also retaining the penguin operator[2] $Q_P = \bar{s}\gamma^\mu_L D^\nu t^A G^A_{\mu\nu} b$ as in ref. [3], one actually does not fully consider the contribution of $Q_3, \ldots, Q_6$. Unfortunately just the insertion of Q_5, Q_6 in the one loop diagrams gives a scheme dependent contribution, which does not vanish in the NDR scheme. Hence NDR calculations using the reduced basis give a regularization dependent result, see ref. [7] and Secs. 3, 5, 7 below.

The coefficients $\vec{C}(\mu)$ of eq. (1) obey the renormalization group equations

$$
\left(-\frac{\partial}{\partial t} + \beta(\alpha_s)\frac{\partial}{\partial \alpha_s} - \frac{\hat{\gamma}^T(\alpha_s)}{2} \right) \vec{C}(t, \alpha_s(t)) = 0, \tag{3}
$$

where $t = \ln(M_W^2/\mu^2)$ and $\alpha_s = g^2/4\pi$. The factor of 2 in eq. (3) normalizes the anomalous dimension matrix as in ref. [15]. $\hat{\gamma}$ includes the contribution

[2]In the "complete" basis this operator can be eliminated via the equations of motion.

due to the renormalization of m_b, the gluon field and the strong coupling constant g, see e.g. refs. [3, 18] (see also Sec. 6).

The initial conditions for the coefficients can be easily found by matching the effective theory with the "full" theory at the scale M_W. They are given by [17]

$$
\begin{aligned}
C_1(M_W) &= 0 \\
C_2(M_W) &= 1 \\
C_3(M_W), \ldots, C_6(M_W) &= 0 \\
C_7(M_W) &= -3\frac{3x^3-2x^2}{2(1-x)^4}\ln x - \frac{8x^3+5x^2-7x}{4(1-x)^3} \\
C_8(M_W) &= -\frac{3x^2}{2(1-x)^4}\ln x + \frac{x^3-5x^2-2x}{4(1-x)^3},
\end{aligned}
\tag{4}
$$

where $x = m_t^2/M_W^2$.

3 Regularization Scheme Independence of the Effective Hamiltonian

In this section the explicit solution of eq. (3) for the coefficients $\vec{C}(\mu)$ is given and the regularization scheme independence of the Effective Hamiltonian is discussed, following ref. [7]. The solution in eq. (7), as well as the relation among matrices in different schemes in eq. (21), rely on the peculiar structure of the anomalous dimension matrix, which is

$$
\hat{\gamma} = \frac{\alpha_s}{4\pi}\begin{pmatrix} \hat{\gamma}_r & \vec{\beta}_7 & \vec{\beta}_8 \\ \vec{0}^T & \gamma_{77} & 0 \\ \vec{0}^T & \gamma_{87} & \gamma_{88} \end{pmatrix}. \tag{5}
$$

This "almost" triangular form is obtained because the magnetic operators Q_7, Q_8 do not mix with the 4-fermion operators $Q_1, \ldots, Q_6$. Then it is convenient to introduce the reduced 6×6 matrix $\hat{\gamma}_r$ which mixes $Q_1, \ldots, Q_6$ among themselves and two 6-component column vectors $\vec{\beta}_7 = (\gamma_{17}, \gamma_{27}, \ldots, \gamma_{67})$ and $\vec{\beta}_8 = (\gamma_{18}, \gamma_{28}, \ldots, \gamma_{68})$, which account for the two-loop mixing of the 4-fermion operators with the magnetic ones.

A very peculiar characteristic of this calculation is that at the LO of the perturbative expansion both one-loop and two-loop diagrams contribute. The mixing of 4-fermion operators among themselves ($\hat{\gamma}_r$) as well as the mixing of magnetic-type operators among themselves (γ_{77}, γ_{87}, γ_{88}) are one-loop effects (at LO), while the mixing between 4-fermion and magnetic-type operators ($\vec{\beta}_7$, $\vec{\beta}_8$) is a two-loop effect (always at LO).

In terms of these quantities the RGE are given by

$$
\begin{aligned}
2\mu^2 \frac{d}{d\mu^2} \vec{C}_r(\mu) &= \frac{\alpha_s}{4\pi} \hat{\gamma}_r^T \vec{C}_r(\mu) \\
2\mu^2 \frac{d}{d\mu^2} C_7(\mu) &= \frac{\alpha_s}{4\pi} \left(\vec{\beta}_7 \cdot \vec{C}_r(\mu) + \gamma_{77} C_7(\mu) + \gamma_{87} C_8(\mu) \right) \\
2\mu^2 \frac{d}{d\mu^2} C_8(\mu) &= \frac{\alpha_s}{4\pi} \left(\vec{\beta}_8 \cdot \vec{C}_r(\mu) + \gamma_{88} C_8(\mu) \right),
\end{aligned}
\tag{6}
$$

where $\vec{C}_r(\mu) = (C_1(\mu), \ldots, C_6(\mu))$, $\alpha_s = \alpha_s(\mu)$ and $\mu^2 d/d\mu^2 = \mu^2 \partial/\partial\mu^2 + \beta(\alpha_s)\partial/\partial\alpha_s$. Diagonalizing the submatrix which mixes the magnetic operators, one obtains

$$
\begin{aligned}
2\mu^2 \frac{d}{d\mu^2} \vec{C}_r(\mu) &= \frac{\alpha_s}{4\pi} \hat{\gamma}_r^T \vec{C}_r(\mu) \\
2\mu^2 \frac{d}{d\mu^2} v_7(\mu) &= \frac{\alpha_s}{4\pi} \gamma_{77} v_7(\mu) \\
2\mu^2 \frac{d}{d\mu^2} v_8(\mu) &= \frac{\alpha_s}{4\pi} \gamma_{88} v_8(\mu),
\end{aligned}
\tag{7}
$$

where

$$
\begin{aligned}
v_7(\mu) &= C_7(\mu) + \vec{\alpha}_7 \cdot \vec{C}_r(\mu) + \frac{\gamma_{87}}{\gamma_{77} - \gamma_{88}} C_8(\mu) \\
v_8(\mu) &= C_8(\mu) + \vec{\alpha}_8 \cdot \vec{C}_r(\mu)
\end{aligned}
\tag{8}
$$

with

$$
\begin{aligned}
\vec{\alpha}_7 &= \left(\gamma_{77} \hat{1} - \hat{\gamma}_r \right)^{-1} \left[\vec{\beta}_7 + \frac{\gamma_{87}}{\gamma_{77} - \gamma_{88}} \vec{\beta}_8 \right] \\
\vec{\alpha}_8 &= \left(\gamma_{88} \hat{1} - \hat{\gamma}_r \right)^{-1} \vec{\beta}_8.
\end{aligned}
\tag{9}
$$

The rhs of eqs. (7) involves only one loop quantities, so that the solutions $\vec{C}_r(\mu)$, $v_7(\mu)$ and $v_8(\mu)$ are independent of the regularization scheme. However the expression of both $v_7(\mu)$ and $v_8(\mu)$, eq. (8), contains both scheme-dependent and -independent quantities. In particular $\vec{C}_r(\mu)$ is the LO solution of the RGE for the 4-fermion operators, which is known to be regularization scheme independent. Indeed, $\vec{C}_r(\mu)$ is known up to next-to-leading order terms [15, 19], which are not to be considered in our LO calculation. On the contrary $\vec{\beta}_7$ and $\vec{\beta}_8$, hence $\vec{\alpha}_7$, $\vec{\alpha}_8$ and $C_7(\mu)$, $C_8(\mu)$, come from two loop diagrams (see Sec. 5 below) and they do depend on regularization scheme, even if they are LO results. Precisely this point, that was missed in refs. [1]-[5], is responsible for the difference between previous results in NDR and DRED schemes, as stressed in ref. [7].

Moreover, already noted in ref. [4], the operators Q_5, Q_6 have non zero matrix elements between the b and $s\gamma$ ($s\,g$) states, through the penguin diagrams in fig. (3) with massive b loop propagators. These one loop matrix elements and the tree level matrix elements of the magnetic operators are of the same order in α_s, so that the matrix elements of the Effective Hamiltonian can be written as

$$\begin{aligned} < s\gamma|H_{eff}|b > &= C_7(\mu) < s\gamma|Q_7(\mu)|b > +C_5(\mu) < s\gamma|Q_5(\mu)|b > \\ &\quad +C_6(\mu) < s\gamma|Q_6(\mu)|b > \\ &= \tilde{C}_7(\mu) < s\gamma|Q_7(\mu)|b > \end{aligned}$$

$$\begin{aligned} < sg|H_{eff}|b > &= C_8(\mu) < sg|Q_8(\mu)|b > +C_5(\mu) < sg|Q_5(\mu)|b > \\ &= \tilde{C}_8(\mu) < sg|Q_8(\mu)|b >, \end{aligned} \tag{10}$$

where the coefficients $\tilde{C}_7(\mu)$, $\tilde{C}_8(\mu)$ are defined as

$$\begin{aligned} \tilde{C}_7(\mu) &= C_7(\mu) + \vec{Z}_7 \cdot \vec{C}_r(\mu) \\ \tilde{C}_8(\mu) &= C_8(\mu) + \vec{Z}_8 \cdot \vec{C}_r(\mu). \end{aligned} \tag{11}$$

Eqs. (10) and (11) can be seen as a finite renormalization of the operators such that the matrix elements of Q_5 and Q_6 vanish. The vectors $\vec{Z}_7$ and $\vec{Z}_8$ can be considered as the effect of a mixing of order α_s^0 among Q_5, Q_6 and the magnetic operators. They are calculated from the finite part of the penguin diagrams in fig. (3), thus they depend on the regularization scheme. We find that they vanish in HV and DRED, while in NDR they are given by

$$\begin{aligned}\vec{Z}_7^{NDR} &= (0,0,0,0,2,2N)\\ \vec{Z}_8^{NDR} &= (0,0,0,0,2,0)\,.\end{aligned} \tag{12}$$

We now show how the scheme independence of the Effective Hamiltonian is recovered. In terms of the operators renormalized at the scale μ, the Effective Hamiltonian is given by

$$\begin{aligned}H_{eff} \sim\; & \vec{Q}_r^T(\mu)\cdot\vec{C}_r(\mu)\\ & +\left\{v_7(\mu)+\left[\left(\hat{\gamma}_r-\gamma_{77}\hat{1}\right)^{-1}\left(\vec{\beta}_7+\frac{\gamma_{87}}{\gamma_{77}-\gamma_{88}}\vec{\beta}_8\right)+\vec{Z}_7\right]\cdot\vec{C}_r(\mu)\right.\\ & \left.+\frac{\gamma_{87}}{\gamma_{88}-\gamma_{77}}\left[v_8(\mu)+\left(\hat{\gamma}_r-\gamma_{88}\hat{1}\right)^{-1}\vec{\beta}_8\cdot\vec{C}_r(\mu)\right]\right\}Q_7(\mu)\\ & +\left\{v_8(\mu)+\left[\left(\hat{\gamma}_r-\gamma_{88}\hat{1}\right)^{-1}\vec{\beta}_8+\vec{Z}_8\right]\cdot\vec{C}_r(\mu)\right\}Q_8(\mu)\\ =\; & \vec{Q}_r^T(\mu)\cdot\vec{C}_r(\mu)\\ & +\left\{v_7(\mu)+\vec{\omega}_7\cdot\vec{C}_r(\mu)+\frac{\gamma_{87}}{\gamma_{88}-\gamma_{77}}\left[v_8(\mu)+\vec{\omega}_8\cdot\vec{C}_r(\mu)\right]\right\}Q_7(\mu)\\ & +\left\{v_8(\mu)+\vec{\omega}_8\cdot\vec{C}_r(\mu)\right\}Q_8(\mu),\end{aligned} \tag{13}$$

where

$$\begin{aligned}\vec{\omega}_7 &= \left(\hat{\gamma}_r-\gamma_{77}\hat{1}\right)^{-1}\left(\vec{\beta}_7+\frac{\gamma_{87}}{\gamma_{77}-\gamma_{88}}\vec{\beta}_8\right)+\vec{Z}_7+\frac{\gamma_{87}}{\gamma_{77}-\gamma_{88}}\vec{Z}_8\\ \vec{\omega}_8 &= \left(\hat{\gamma}_r-\gamma_{88}\hat{1}\right)^{-1}\vec{\beta}_8+\vec{Z}_8.\end{aligned} \tag{14}$$

Thus the Effective Hamiltonian is scheme independent provided that $\vec{\omega}_7$ and $\vec{\omega}_8$ do not change with the scheme. We will prove in the following that this is indeed the case.

Now we discuss the change in the anomalous dimension matrix induced by a change of the regularization scheme. The anomalous dimension matrix in a given scheme "a" is defined as

$$\hat{\gamma}^a = 2\left(\hat{Z}^a(\mu)\right)^{-1}\mu^2\frac{d}{d\mu^2}\hat{Z}^a(\mu), \tag{15}$$

where $\hat{Z}^a$ is the matrix of the renormalization constants which gives the renormalized operators in terms of the bare ones

$$\vec{Q}(\mu) = \left(\hat{Z}^a\right)^{-1} \vec{Q}_B. \tag{16}$$

Let us consider different renormalization schemes. The operators renormalized through the usual $\overline{MS}$ subtraction change from one scheme to another. In order to have the same renormalized operators in all the schemes, one can define them using the $\overline{MS}$ procedure in a given scheme and then adopt a suitable non-minimal subtraction in the other ones. So the $\overline{MS}$ renormalization constants in two different schemes "a" and "b" can be related through the equation

$$\hat{Z}^a = \hat{Z}^b \hat{r}, \tag{17}$$

where the matrix $\hat{r}$ accounts for the change of the subtraction procedure in the scheme "b" necessary to define operators renormalized as in the scheme "a". In our case the matrix $\hat{r}$ is expressed in terms of the vectors $\vec{Z}_{7,8}$ introduced in eq. (11), as discussed in the following.

The relation between the anomalous dimension matrices in the schemes "a" and "b" is easily obtained from eqs. (15)-(17)

$$\hat{\gamma}^a = \hat{r}^{-1}\hat{\gamma}^b\hat{r}. \tag{18}$$

This relation was already found in ref. [19] and applied to the next-to-leading calculation of the $\Delta S = 1$ Effective Hamiltonian. In that case $\hat{r}$ deviated from $\hat{1}$ by terms of order α_s. Here we are not interested in such terms, but now, as a consequence of eqs. (10)-(12), $\hat{r}$ differs from the identity already at order α_s^0. However, due to the peculiar form of the anomalous dimension matrix discussed above, the matrix $\hat{r}$ is simply

$$\hat{r} = \begin{pmatrix} \hat{1}_6 & -\Delta\hat{Z} \\ 0 & \hat{1}_2 \end{pmatrix}, \tag{19}$$

where $\hat{1}_{6,2}$ are 6×6 and 2×2 identity matrices and $\Delta\hat{Z}$ is a 6×2 matrix. Imposing the condition that the renormalized operators coincide in the two schemes, $\Delta\hat{Z}$ is defined as the difference of the vectors $\vec{Z}_{7,8}$ of eq. (11) calculated in the two different regularization schemes, i.e. $\Delta\hat{Z} = (\vec{Z}_7^a - \vec{Z}_7^b, \vec{Z}_8^a - \vec{Z}_8^b)$.

At the order we are interested in, eq. (18) gives

$$\Delta\hat{\gamma} = \hat{\gamma}^a - \hat{\gamma}^b = [\Delta\hat{Z}, \hat{\gamma}^b] - \Delta\hat{Z}\hat{\gamma}^b\Delta\hat{Z}. \tag{20}$$

Contrary to the already mentioned $\Delta S = 1$ case, eq. (20) does not define a scheme independent combination of the one and two loop matrices, namely it can not be written just in terms of quantities which are either calculated as differences between the two schemes or scheme independent by themselves. However a scheme independent combination actually exists due to the structure of the matrices. In fact, applying eq. (20) to anomalous dimension matrices of the form of eq. (5), we find

$$\begin{aligned}
\hat{\gamma}^a_r &= \hat{\gamma}^b_r = \hat{\gamma}_r \\
(\Delta\vec{\beta}_7)_j = \Delta\gamma_{j7} &= \left[\left(\gamma_{77}\hat{1} - \hat{\gamma}_r\right)\Delta\vec{Z}_7 + \gamma_{87}\Delta\vec{Z}_8\right]_j \\
(\Delta\vec{\beta}_8)_j = \Delta\gamma_{j8} &= \left[\left(\gamma_{88}\hat{1} - \hat{\gamma}_r\right)\Delta\vec{Z}_8\right]_j,
\end{aligned} \tag{21}$$

where $j = 1, \ldots, 6$. This clearly implies that the combinations

$$\begin{aligned}
&\vec{\beta}_7 - \left(\gamma_{77}\hat{1} - \hat{\gamma}_r\right)\vec{Z}_7 - \gamma_{87}\vec{Z}_8 \\
&\vec{\beta}_8 - \left(\gamma_{88}\hat{1} - \hat{\gamma}_r\right)\vec{Z}_8
\end{aligned} \tag{22}$$

are scheme independent. Using eqs. (21), one can easily check that the combinations $\vec{\omega}_7$, $\vec{\omega}_8$ in eq. (14) give $\Delta\vec{\omega}_{7,8} = 0$, i.e. they are scheme independent too. In turn this implies that, as expected, the Effective Hamiltonian, eq. (13), is independent of the regularization scheme.

Eqs. (21) can be used to relate classes of diagrams calculated in different schemes. Thus it can be a useful check of the calculation, see Sec. 5 below.

4 Dimensional Regularization Schemes

In this section we briefly recall the definitions of the regularization procedures we have used for our calculations. Other nice discussions can be found in refs. [20, 21] and references therein, while for more details the reader should refer to the literature on the specific subject.

The regularization procedures we have used, NDR, HV and DRED, are all based on the dimensional regularization of the loop integrals [10], which consists in performing the integration over the loop momenta in D dimensions, thus turning the divergences into regularized $1/(4-D)$ pole terms. The extension of the Dirac algebra to non-integer dimensions presents no difficulty except for the properties of traces involving γ_5 and in general expressions containing the completely antisymmetric tensor $\epsilon_{\mu\nu\rho\sigma}$, which does not have any meaningful extension in D dimensions. Actually the three schemes differ from each other in the way they treat γ_5. Another relevant point is that the relation

$$\gamma_\mu\gamma_\nu\gamma_\rho = \gamma_\mu g_{\nu\rho} - \gamma_\nu g_{\mu\rho} + \gamma_\rho g_{\mu\nu} - i\gamma^\sigma\gamma_5\epsilon_{\mu\nu\rho\sigma} \tag{23}$$

which, in 4 dimensions, projects the product of three γ matrices on the basis does not hold in D dimensions. This implies that more complicated tensor structures, which eventually vanish in 4 dimensions, appear in the regularized theory and must be considered in the renormalization procedure.

Let us now separately discuss how the three schemes are implemented.

4.1 Naive Dimensional Regularization

In NDR all the Lorentz indices appearing in the regularized theory are assumed to be in D dimensions. The Dirac algebra is identical to the 4-dimensional one, including the properties of γ_5, once the 4-dimensional metric tensor is replaced by the D-dimensional one. The definitions we are interested in are simply

$$\begin{aligned} g_{\mu\nu}g^{\mu\nu} &= D \\ \{\gamma_\mu, \gamma_5\} &= 0. \end{aligned} \tag{24}$$

Obviously, since the completely antisymmetric tensor is not defined in D-dimensions, traces involving odd number of γ_5 are ill-defined too. However, to our knowledge, once the problem is properly fixed, there is no calculation which shows a failure of this scheme. Our way to fix the γ_5 problem is the one implemented by Schoonschip [22], which defines traces of odd number of γ_5 in NDR in the same way they are defined in the HV scheme, see below.

4.2 't Hooft-Veltman Regularization

In HV [10], Lorentz indices in D, 4 and $(D-4)$ dimensions are introduced, together with the corresponding metric tensors $g_{\mu\nu}$, $\tilde{g}_{\mu\nu}$ and $\hat{g}_{\mu\nu}$. All the γ matrices are taken in D dimension, then indices are split in 4 and $(D-4)$ components, according to the rules

$$\begin{aligned} g_{\mu\nu} &= \tilde{g}_{\mu\nu} + \hat{g}_{\mu\nu} \\ \tilde{g}_{\mu\nu}\tilde{g}^{\mu\nu} = 4 \quad &, \quad \hat{g}_{\mu\nu}\hat{g}^{\mu\nu} = D-4 \\ \tilde{g}_{\mu\nu}\hat{g}^{\nu\rho} &= 0. \end{aligned} \tag{25}$$

These rules define also the extended Dirac algebra, once one notes that γ matrices in 4 ($\tilde{\gamma}^{\mu}$) and $(D-4)$ ($\hat{\gamma}^{\mu}$) dimensions can be written in terms of D dimensional matrices as $\tilde{g}^{\mu\nu}\gamma_{\nu}$ and $\hat{g}^{\mu\nu}\gamma_{\nu}$ respectively and the usual commutation relations among the D-dimensional Dirac matrices in terms of the D-dimensional metric tensor $g^{\mu\nu}$ are assumed.

γ matrices in D dimensions do not have definite commutation relation with γ_5. In fact the following relations hold in HV

$$\{\tilde{\gamma}_{\mu}, \gamma_5\} = 0 \qquad , \qquad [\hat{\gamma}_{\mu}, \gamma_5] = 0. \tag{26}$$

This is equivalent to define γ_5 as the product $i\tilde{\gamma}_0\tilde{\gamma}_1\tilde{\gamma}_2\tilde{\gamma}_3$. This way of treating γ_5 in D dimensions is the only known one which does not give rise to algebraic inconsistencies or introduce ill-defined quantities. On the other hand, due to the splitting of indices, the HV scheme is the most difficult to handle among the three considered here as far as the algebraic manipulation problems are concerned.

Finally we mention that the chiral vertices in D dimensions can be defined in different ways, all having the same limit when D tends to 4 dimensions. We use the symmetrized form

$$\frac{1}{2}(V \pm A)\gamma_{\mu}(V \pm A) = \tilde{\gamma}_{\mu}(V \pm A). \tag{27}$$

In this way the bare vertices preserve the chirality of the external fields also in D dimensions.

4.3 Dimensional Reduction

In DRED [8] the Dirac matrices have indices in 4 dimensions only, thus the algebra is greatly simplified. The D-dimensional indices are introduced by the loop integrals, which generate the D-dimensional metric tensor $g_{\mu\nu}$, so that γ_μ in D dimensions is given by $g_\mu^\nu \tilde{\gamma}_\nu$. The basic rules

$$\begin{aligned} \tilde{g}_{\mu\nu} &= g_{\mu\nu} + \hat{g}_{\mu\nu} \\ g_{\mu\nu}g^{\mu\nu} = D \quad &, \quad \hat{g}_{\mu\nu}\hat{g}^{\mu\nu} = 4 - D \\ g_{\mu\nu}\hat{g}^{\nu\rho} &= 0 \end{aligned} \tag{28}$$

are formally similar to the HV ones provided the roles of $g_{\mu\nu}$ and $\tilde{g}_{\mu\nu}$ are exchanged, but, contrary to that case, DRED is known to be algebraically inconsistent [23]. Moreover one should also mention that DRED fails to reproduce the triangle anomaly, unless further ad-hoc prescriptions are assumed [24]. Finally it is well known that one has to take care of many theoretical subtleties regarding the renormalization of operators, living in $(4-D)$ dimensions, when higher order calculations are performed [21].

In spite of all these problems, no calculation, with the exception of the triangle anomaly, gives so far a wrong result. Concerning our calculation, neither inconsistencies of the regularization scheme nor other problems with the renormalization procedure in D dimensions show out, once a suitable definition of the $(4-D)$-dimensional operators is introduced, as explained in Sec. 5.

5 Diagrams and Counter-terms

In this section the main results of our study are given. Contributions from the one and two loop Feynman diagrams in figs. (1)- (4) to the anomalous dimension matrix are presented in the three considered regularization schemes. Tabs. (1)-(10) contain the results of these diagrams in terms of the coefficients of the poles in the number of dimensions, appearing as powers of $1/\epsilon = 2/(4-D)$.

5.1 One Loop Diagrams

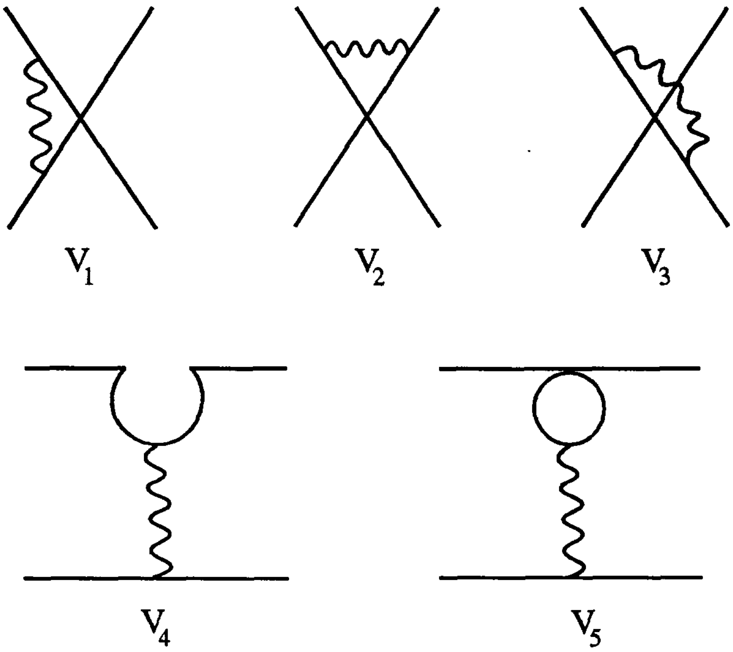

Figure 1: One loop diagrams which generate both the 4-fermion operator mixing and the counter-terms to be used in the two loop calculation.

Let us start with the $O(\alpha_s^0)$ finite mixing among 4-fermion and magnetic operators, already discussed in Sec. 3. The penguin diagrams in fig. (3) could mix 4-fermion operator with magnetic ones. The coupling constant is re-absorbed in the definition of the magnetic operators, so this mixing appears already at $O(\alpha_s^0)$. However penguin diagrams in HV and DRED have neither pole nor finite parts on the magnetic form factor. Differently in NDR, when massive quark fields propagate in the loop, the diagram $P1$ induces a finite mixing among Q_5, Q_6 and Q_7, Q_8. In fact the calculation of $P1$ with a $\gamma_L^\mu \otimes \gamma_{\mu R}$ vertex insertion gives

$$2m_b\,(\not{q}\gamma_\mu - \gamma_\mu\not{q}))\,(1+\gamma_5)\,. \tag{29}$$

diagram	M	$\gamma_L^\mu \otimes \gamma_{\mu L}$	$\gamma_L^\mu \otimes \gamma_{\mu R}$
		$(1/\epsilon)$	$(1/\epsilon)$
V_1	2	1	1
V_2	2	-4	-1
V_3	2	1	4
V_4	1	-4/3	-
V_5	1	-4/3	-4/3

Table 1: Singular parts of the diagrams in figs. (1), with a $\gamma_L^\mu \otimes \gamma_{\mu L}$ or a $\gamma_L^\mu \otimes \gamma_{\mu R}$ vertex insertion. V_1-V_3 results are proportional to the inserted 4-fermion structures. V_4-V_5 are proportional to $\gamma_L^\mu \otimes \gamma_\mu$. The multiplicity of the diagrams is also reported in the table. Colour factors and $\alpha_s/4\pi$ are omitted.

Selecting the magnetic form factor through the projection

$$m_b(1+\gamma_5)\not{q}\tilde{\gamma}_\mu \rightarrow \frac{1}{2}, \qquad m_b(1+\gamma_5)\tilde{\gamma}_\mu\not{q} \rightarrow -\frac{1}{2}, \tag{30}$$

the values of the vector $\vec{Z}$ in eq. (12) can be readily obtained. The accidental vanishing of $\vec{Z}$ in both the HV and DRED schemes makes them to give coincident results even at intermediate stages of the calculation.

Figs. (1) and (2) show all the diagrams required to calculate at the leading order the 4-fermion operator mixing matrix $\hat{\gamma}_r$ and the mixing of the magnetic operators among themselves. The corresponding results can be found in tabs. (1) and (2), where the pole coefficients are reported. These results, which do not depend on the regularization scheme, are established since a long time [18, 25], thus we omit the details on their calculation. Our results, as well as the corresponding anomalous dimension sub-matrices in eqs. (43) and (44), coincide with those of refs. [25] and [18]. We just mention that the gauge dependence of the diagrams M_1-M_5 cancels out when the external gluon field renormalization, see eqs. (37)-(38), is taken into account.

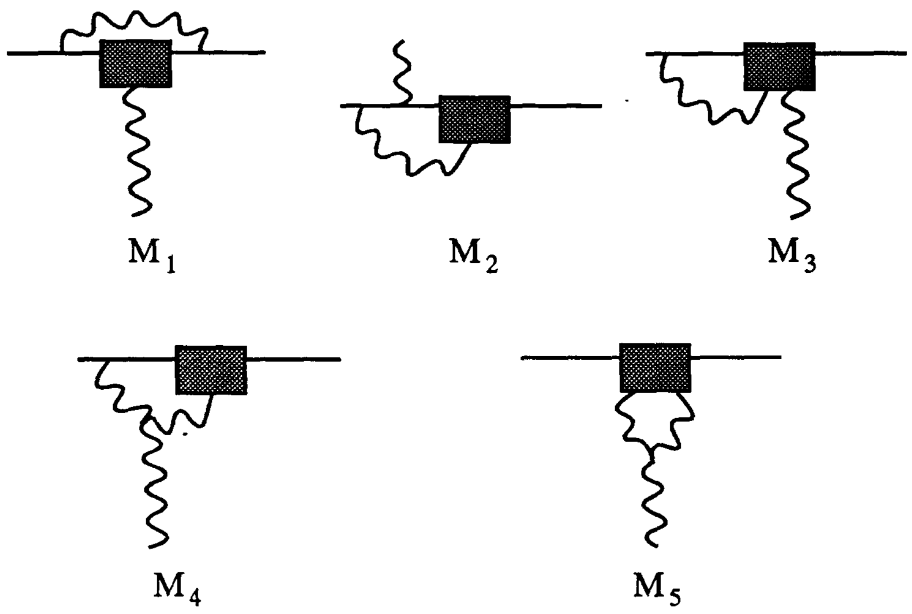

Figure 2: Diagrams responsible for the one loop renormalization of the magnetic operators.

5.2 One Loop Counter-terms

Counter-terms to be inserted in the two loop diagrams are obtained from the diagrams in figs. (1)-(3). Many scheme dependent operators, which vanish in 4 dimensions, are generated along with the usual counter-terms proportional to the operators already present in the 4-dimensional basis. It is well known [15, 20, 21] that "effervescent" operators must be considered in the renormalization procedure, namely they must be properly inserted as counter-terms in the two loop diagrams, in order to have the right final result.

Here we do not repeat the procedure to define these operators in HV and NDR, since it is fully explained in refs. [15, 19, 20]. Also the DRED "effervescent" operators generated by the 4-fermion diagrams in fig. (1) are known from ref. [21]. We confirm all previous results and give some details

Diagram	$1/\epsilon$
M_1	—
M_2	-4
M_3	-1
M_4	6
M_4^{bg}	5
M_5	$-\frac{3}{2}$
M_5^{bg}	-2

Table 2: Singular parts of the diagrams in fig. (2). All the results are proportional to the magnetic operators. The factor $\alpha_s/4\pi$ is omitted. The diagrams M_4 and M_5 are calculated both in the Feynman and background gauges.

only on our DRED calculation of the "effervescent" operators due to the penguin and gluon-photon diagrams in fig. (3), recently presented also in ref. [11].

Contrary to other schemes, in DRED the γ algebra is performed in 4 dimensions so that no complicated tensor structure appears and the "effervescent" operators can be readily defined by inspection as those terms that have $(4-D)$-dimensional Lorentz indices saturated on the external fields. The "effervescent" part of the penguin diagrams in DRED is then given by

$$-\frac{2}{3}\frac{1}{\epsilon}q^2\hat{g}^{\mu\nu}\gamma_\nu(1-\gamma_5)\,. \tag{31}$$

This result coincides with the corresponding one of ref. [11].

Concerning the diagrams $P_{VV}(a)$ and $P_{VV}(b)$ in fig. (3), their "effervescent" parts are found to be respectively

$$\begin{aligned} &-\frac{2}{3\epsilon}(q+2l)^\mu\gamma_\nu\hat{g}^{\nu\rho}(1-\gamma_5)+\frac{1}{\epsilon}\left(\not{q}\gamma^\mu-\gamma^\mu\not{q}\right)\gamma_\nu\hat{g}^{\nu\rho}(1-\gamma_5)+\dots \\ &\frac{2}{3\epsilon}(q+2l)^\mu\gamma_\nu\hat{g}^{\nu\rho}(1-\gamma_5)+\frac{1}{\epsilon}\left(\not{q}\gamma^\mu-\gamma^\mu\not{q}\right)\gamma_\nu\hat{g}^{\nu\rho}(1-\gamma_5)+\dots \end{aligned} \tag{32}$$

The dots indicates further terms that can be omitted since they contribute only to the "effervescent" part of the two loop diagrams. By summing the

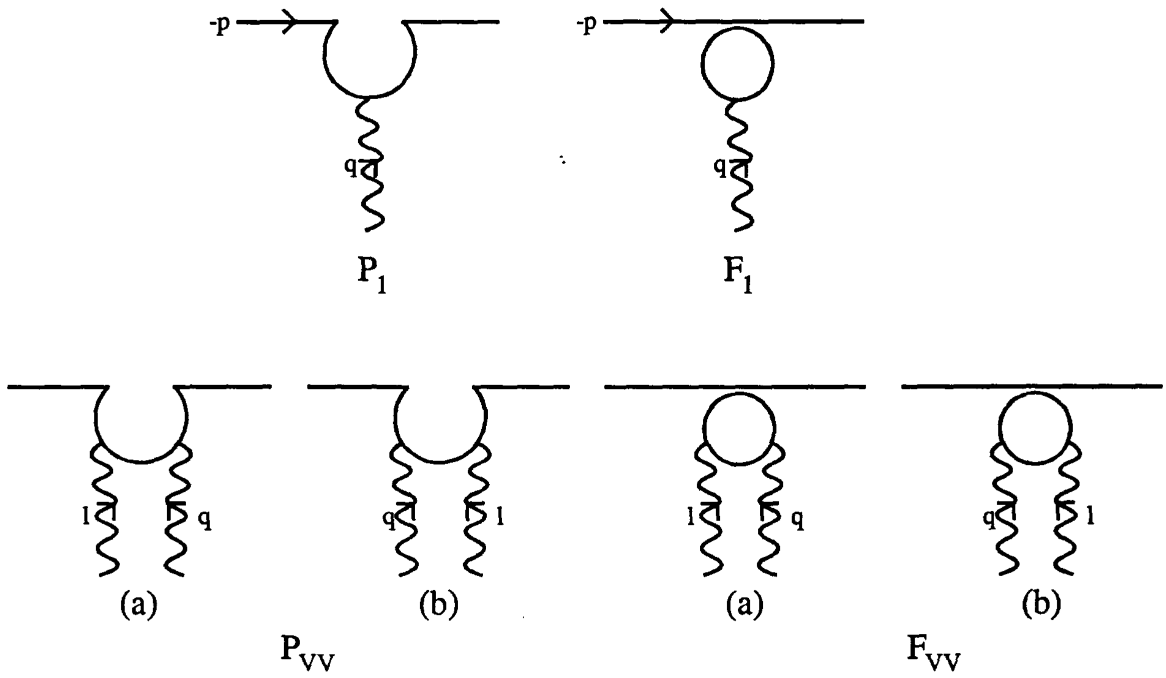

Figure 3: Diagrams which generate the counter-terms discussed in the text. In DRED they generate "effervescent" contributions that cannot be omitted.

two terms in eq. (32), we obtain a counter-term in agreement with the one presented in ref. [11], once the charge of the c quark and the different normalization of the operators are taken into account[3].

It is worthwhile to note that, as shown in ref. [15], the insertions of the counter-terms generated by the diagrams P_{VV} and F_{VV} in fig. (3) and by the longitudinal parts of the penguin diagrams vanish, so that one can retain 4-fermion operators only as counter-terms in the Hamiltonian. However in DRED the diagrams of fig. (3) give "effervescent" contributions that must be taken into account.

[3]We thank M. Misiak for clarifying this point.

5.3 Two Loop Diagrams

The relevant two loop diagrams are shown in fig. (4) and the corresponding results in the three considered regularization schemes can be found in tabs. (3)-(10), which contain the pole coefficients of the diagrams projected on the magnetic form factor. Two tables for each different kind of Dirac structure inserted in the upper vertex are presented. The first one contains the pole coefficients of the bare diagram (D), the insertion of 4-dimensional counter-terms (C) and the insertion of "effervescent" counter-terms (E). The second one collects the final results of the renormalized diagrams ($\overline{D}$), obtained as

$$\overline{D} = D - C - \frac{1}{2}E, \tag{33}$$

see eq. (41) below. Results from the insertion of a $\gamma_L^\mu \otimes \gamma_{\mu L}$ upper vertex in the P-type diagrams of fig. (4) are reported in tabs. (3)-(4). Those coming from $\gamma_L^\mu \otimes \gamma_{\mu L}$ insertion in F-type diagrams can be found in tabs. (5)-(6). $\gamma_L^\mu \otimes \gamma_{\mu R}$ 4-fermion vertex, inserted in P- and F-type diagrams, originate the results in tabs. (7)-(8) and (9)-(10) respectively. Note that the left-right operator insertion in the P-type diagrams, tab. (7), does not vanish just because of the massive loop propagators, thus these diagrams contribute only when $q = b$ is taken in Q_5, Q_6.

The calculation of the two loop diagrams results in many tensor structures, containing m_b mass and/or external momenta. Further projections are required, besides those in eq. (30)

$$\begin{aligned}
m_b(1+\gamma_5)\tilde{\gamma}^\mu \not{p} \to 0 \quad &, \quad m_b(1+\gamma_5)\not{p}\tilde{\gamma}^\mu \to \frac{1}{2} \\
m_b(1+\gamma_5)\frac{\not{p}\not{q}}{q^2}q^\mu \to 0 \quad &, \quad m_b(1+\gamma_5)\frac{\not{p}\not{q}}{q^2}p^\mu \to \frac{1}{4} \\
m_b(1+\gamma_5)\frac{\not{q}\not{p}}{q^2}q^\mu \to 0 \quad &, \quad m_b(1+\gamma_5)\frac{\not{q}\not{p}}{q^2}p^\mu \to 0 \\
m_b(1+\gamma_5)p^\mu \to \frac{1}{4} \quad &, \quad m_b(1+\gamma_5)q^\mu \to 0 \\
(1+\gamma_5)\not{q}q^\mu \to 0 \quad &, \quad (1+\gamma_5)\not{q}p^\mu \to -\frac{1}{4} \\
(1+\gamma_5)\not{p}q^\mu \to 0 \quad &, \quad (1+\gamma_5)\not{p}p^\mu \to -\frac{1}{4}.
\end{aligned} \tag{34}$$

Moreover in DRED also the antisymmetric tensor $\epsilon_{\mu\nu\rho\sigma}$ appears, either in pure 4-dimensional expressions or in tensors involving $\hat{g}_{\mu\nu}$. In these cases the projections are

$$
\begin{aligned}
m_b(1+\gamma_5)\tilde{\gamma}_\nu\tilde{\gamma}_\rho\epsilon^{\mu\nu\rho\sigma}q_\sigma &\rightarrow 1 \\
m_b(1+\gamma_5)\tilde{\gamma}_\nu\tilde{\gamma}_\rho\epsilon^{\mu\nu\rho\sigma}p_\sigma &\rightarrow \frac{1}{2} \\
m_b(1+\gamma_5)\tilde{\gamma}_\alpha\tilde{\gamma}_\rho\hat{g}^\alpha_\nu\epsilon^{\mu\nu\rho\sigma}q_\sigma &\rightarrow \frac{1}{2}(4-D) \\
m_b(1+\gamma_5)\tilde{\gamma}_\alpha\tilde{\gamma}_\rho\hat{g}^\alpha_\nu\epsilon^{\mu\nu\rho\sigma}p_\sigma &\rightarrow \frac{1}{4}(4-D) \\
(1+\gamma_5)\tilde{\gamma}_\nu\epsilon^{\mu\nu\rho\sigma}q_\rho p_\sigma &\rightarrow \frac{1}{4} \\
(1+\gamma_5)\tilde{\gamma}_\alpha\hat{g}^\alpha_\nu\epsilon^{\mu\nu\rho\sigma}q_\rho p_\sigma &\rightarrow \frac{1}{4}(4-D). \qquad (35)
\end{aligned}
$$

Let us consider now the relations among different schemes. Eqs. (21) enforce a set of relations among one and two loop diagrams, which can be easily obtained by considering how each diagram contributes to the anomalous dimension matrix (i.e. its Dirac and colour structure). These relations are

$$
\begin{aligned}
&\Delta(P_2+P_3)=0, \qquad \Delta(F_2+F_3)=0 \\
&\Delta(P_2+P_4)=0, \qquad \Delta(F_2+F_4)=0 \\
&\Delta P_7=-\frac{1}{4}P_1\Delta P_1^{m_b}, \qquad \Delta F_7=-\frac{1}{4}F_1\Delta P_1^{m_b} \\
&\Delta(P_2^{m_b}+P_3^{m_b}+P_5^{m_b}+P_7^{m_b}+P_8^{m_b}+P_9^{m_b})=-7\Delta P_1^{m_b} \\
&\Delta(P_5^{m_b}+P_8^{m_b}+P_9^{m_b})=-5\Delta P_1^{m_b} \\
&\Delta(P_2^{m_b}+P_4^{m_b}+P_6^{m_b}+P_8^{m_b})=-2\Delta P_1^{m_b}, \qquad (36)
\end{aligned}
$$

where Δ indicates the difference between two different regularization schemes. Quantities denoted by m_b refer to the results of the left-right P-type diagrams with a mass insertion into the loop propagators. They can be found in tab. (8), with the exception of $P_1^{m_b}$, which is equal to 2 in NDR and vanishes in the other two schemes. As already noted, HV and DRED calculations coincide diagram by diagram, so that eqs. (36) are not really interesting.

However, when comparing HV or DRED with NDR, this check is effective and one can verify that all our diagrams satisfy eqs. (36).

Among the other checks passed by our results, one can readily verify

- the cancellation of all the double poles, as an indication that this is a leading order calculation, see eqs. (41);
- the usual relation between the double poles of the bare diagram and the insertion of the counter-terms, the second being two times larger then the first one;
- the gauge independence, checked by using the Feynman and the background gauges [26].

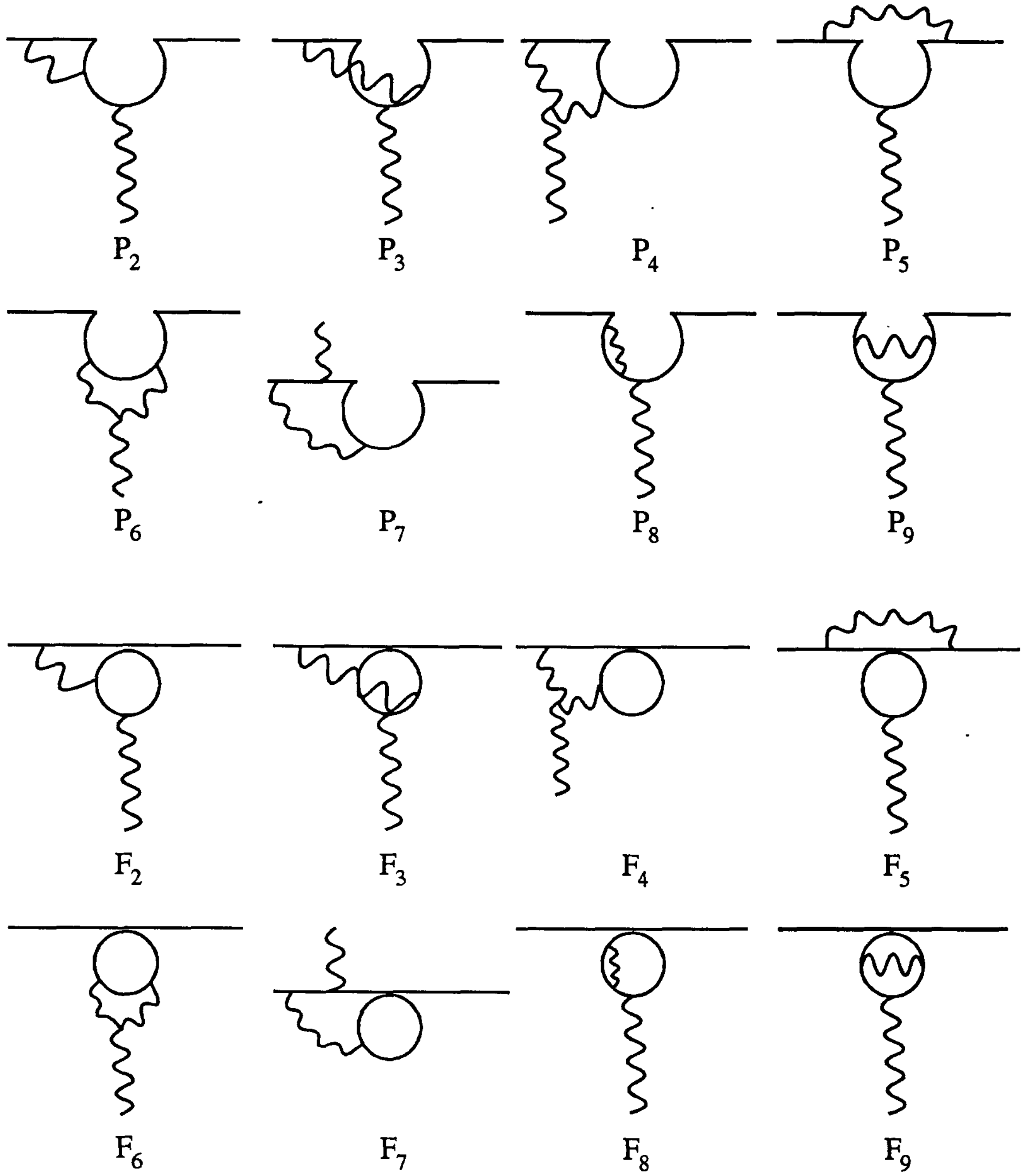

Figure 4: The two loop diagrams relevant for the calculation of the vectors $\vec{\beta}_{7,8}$ in eq. (5).

	D				C				E		
T_N	$\frac{1}{\epsilon^2}$	$\frac{1}{\epsilon}^{HV}$	$\frac{1}{\epsilon}^{NDR}$	$\frac{1}{\epsilon}^{DRED}$	$\frac{1}{\epsilon^2}$	$\frac{1}{\epsilon}^{HV}$	$\frac{1}{\epsilon}^{NDR}$	$\frac{1}{\epsilon}^{DRED}$	$\frac{1}{\epsilon}^{HV}$	$\frac{1}{\epsilon}^{NDR}$	$\frac{1}{\epsilon}^{DRED}$
P_2	$-\frac{1}{9}$	$-\frac{91}{54}$	$-\frac{97}{54}$	$-\frac{29}{27}$	$-\frac{2}{9}$	$-\frac{10}{27}$	$-\frac{22}{27}$	$-\frac{10}{27}$	—	—	$\frac{11}{9}$
P_3	$\frac{1}{9}$	$-\frac{71}{54}$	$-\frac{65}{54}$	$-\frac{25}{27}$	$\frac{2}{9}$	$\frac{10}{27}$	$\frac{22}{27}$	$\frac{10}{27}$	—	—	$\frac{7}{9}$
P_4	$\frac{1}{9}$	$\frac{25}{54}$	$\frac{31}{54}$	$\frac{19}{54}$	$\frac{2}{9}$	$\frac{10}{27}$	$\frac{22}{27}$	$\frac{10}{27}$	—	—	$-\frac{2}{9}$
P_4^{bg}	$\frac{1}{9}$	$\frac{25}{54}$	$\frac{31}{54}$	$\frac{19}{54}$	$\frac{2}{9}$	$\frac{10}{27}$	$\frac{22}{27}$	$\frac{10}{27}$	—	—	$-\frac{2}{9}$
P_7	—	$-\frac{2}{9}$	$-\frac{8}{9}$	$\frac{1}{9}$	—	—	$-\frac{4}{3}$	—	—	—	$\frac{2}{3}$

Table 3: Singular parts of the P diagrams in fig. (4) with a $\gamma_L^\mu \otimes \gamma_{\mu L}$ vertex insertion. The common double poles and the single poles, calculated in HV, NDR and DRED, are presented for the bare diagrams (D), the 4-dimensional (C) and the "effervescent" (E) counter-terms. All the results are proportional to the magnetic operators. Diagram P_4 is calculated both in the Feynman and background gauges.

	$\overline{D}$			
T_N	$\frac{1}{\epsilon^2}$	$\frac{1}{\epsilon}^{HV}$	$\frac{1}{\epsilon}^{NDR}$	$\frac{1}{\epsilon}^{DRED}$
P_2	$\frac{1}{9}$	$-\frac{71}{54}$	$-\frac{53}{54}$	$-\frac{71}{54}$
P_3	$-\frac{1}{9}$	$-\frac{91}{54}$	$-\frac{109}{54}$	$-\frac{91}{54}$
P_4	$-\frac{1}{9}$	$\frac{5}{54}$	$-\frac{13}{54}$	$\frac{5}{54}$
P_4^{bg}	$-\frac{1}{9}$	$\frac{5}{54}$	$-\frac{13}{54}$	$\frac{5}{54}$
P_7	—	$-\frac{2}{9}$	$\frac{4}{9}$	$-\frac{2}{9}$

Table 4: Singular parts of the renormalized P diagrams in fig. (4) with a $\gamma_L^\mu \otimes \gamma_{\mu L}$ vertex insertion. These results are obtained from tab. (3) using eq. (33).

	D				C				E		
T_N	$\frac{1}{\epsilon^2}$	$\frac{1}{\epsilon}^{HV}$	$\frac{1}{\epsilon}^{NDR}$	$\frac{1}{\epsilon}^{DRED}$	$\frac{1}{\epsilon^2}$	$\frac{1}{\epsilon}^{HV}$	$\frac{1}{\epsilon}^{NDR}$	$\frac{1}{\epsilon}^{DRED}$	$\frac{1}{\epsilon}^{HV}$	$\frac{1}{\epsilon}^{NDR}$	$\frac{1}{\epsilon}^{DRED}$
F_2	$-\frac{1}{9}$	$-\frac{91}{54}$	$-\frac{103}{54}$	$-\frac{29}{27}$	$-\frac{2}{9}$	$-\frac{10}{27}$	$-\frac{22}{27}$	$-\frac{10}{27}$	—	—	$\frac{11}{9}$
F_3	$\frac{1}{9}$	$-\frac{71}{54}$	$-\frac{59}{54}$	$-\frac{25}{27}$	$\frac{2}{9}$	$\frac{10}{27}$	$\frac{22}{27}$	$\frac{10}{27}$	—	—	$\frac{7}{9}$
F_4	$\frac{1}{9}$	$\frac{25}{54}$	$\frac{37}{54}$	$\frac{19}{54}$	$\frac{2}{9}$	$\frac{10}{27}$	$\frac{22}{27}$	$\frac{10}{27}$	—	—	$-\frac{2}{9}$
F_4^{bg}	$\frac{1}{9}$	$\frac{25}{54}$	$\frac{37}{54}$	$\frac{19}{54}$	$\frac{2}{9}$	$\frac{10}{27}$	$\frac{22}{27}$	$\frac{10}{27}$	—	—	$-\frac{2}{9}$
F_7	—	$-\frac{2}{9}$	$-\frac{8}{9}$	$\frac{1}{9}$	—	—	$-\frac{4}{3}$	—	—	—	$\frac{2}{3}$

Table 5: The same as tab. (3) for the F diagrams with a $\gamma_L^\mu \otimes \gamma_{\mu L}$ vertex insertion.

	$\overline{D}$			
T_N	$\frac{1}{\epsilon^2}$	$\frac{1}{\epsilon}^{HV}$	$\frac{1}{\epsilon}^{NDR}$	$\frac{1}{\epsilon}^{DRED}$
F_2	$\frac{1}{9}$	$-\frac{71}{54}$	$-\frac{59}{54}$	$-\frac{71}{54}$
F_3	$-\frac{1}{9}$	$-\frac{91}{54}$	$-\frac{103}{54}$	$-\frac{91}{54}$
F_4	$-\frac{1}{9}$	$\frac{5}{54}$	$-\frac{7}{54}$	$\frac{5}{54}$
F_4^{bg}	$-\frac{1}{9}$	$\frac{5}{54}$	$-\frac{7}{54}$	$\frac{5}{54}$
F_7	—	$-\frac{2}{9}$	$\frac{4}{9}$	$-\frac{2}{9}$

Table 6: The same as tab. (4) for the F diagrams with a $\gamma_L^\mu \otimes \gamma_{\mu L}$ vertex insertion.

	D				C				E		
T_N	$\frac{1}{\epsilon^2}$	$\frac{1}{\epsilon}^{HV}$	$\frac{1}{\epsilon}^{NDR}$	$\frac{1}{\epsilon}^{DRED}$	$\frac{1}{\epsilon^2}$	$\frac{1}{\epsilon}^{HV}$	$\frac{1}{\epsilon}^{NDR}$	$\frac{1}{\epsilon}^{DRED}$	$\frac{1}{\epsilon}^{HV}$	$\frac{1}{\epsilon}^{NDR}$	$\frac{1}{\epsilon}^{DRED}$
P_2	—	2	3	2	—	—	4	—	—	—	—
P_3	—	2	-7	2	—	—	-20	—	—	16	—
P_4	—	—	-6	—	—	—	—	—	—	—	—
P_4^{bg}	—	—	-5	—	—	—	—	—	—	—	—
P_5	—	—	—	—	—	—	—	—	—	8	—
P_6	—	—	—	—	—	—	-6	—	—	—	—
P_6^{bg}	—	—	3	—	—	—	-2	—	—	—	—
P_7	—	$-\frac{2}{3}$	-4	—	—	—	—	—	$-\frac{4}{3}$	—	—
P_8	—	—	1	—	—	—	2	—	—	—	—
P_9	—	—	1	—	—	—	2	—	—	8	—

Table 7: The same as tab. (3) for the P diagrams with a $\gamma_L^\mu \otimes \gamma_{\mu R}$ vertex insertion.

	$\overline{D}$			
T_N	$\frac{1}{\epsilon^2}$	$\frac{1}{\epsilon}^{HV}$	$\frac{1}{\epsilon}^{NDR}$	$\frac{1}{\epsilon}^{DRED}$
P_2	—	2	-1	2
P_3	—	2	5	2
P_4	—	—	-6	—
P_4^{bg}	—	—	-5	—
P_5	—	—	-4	—
P_6	—	—	6	—
P_6^{bg}	—	—	5	—
P_7	—	—	-4	—
P_8	—	—	-1	—
P_9	—	—	-5	—

Table 8: The same as tab. (4) for the P diagrams with a $\gamma_L^\mu \otimes \gamma_{\mu R}$ vertex insertion.

	D				C				E		
T_N	$\frac{1}{\epsilon^2}$	$\frac{1}{\epsilon}^{HV}$	$\frac{1}{\epsilon}^{NDR}$	$\frac{1}{\epsilon}^{DRED}$	$\frac{1}{\epsilon^2}$	$\frac{1}{\epsilon}^{HV}$	$\frac{1}{\epsilon}^{NDR}$	$\frac{1}{\epsilon}^{DRED}$	$\frac{1}{\epsilon}^{HV}$	$\frac{1}{\epsilon}^{NDR}$	$\frac{1}{\epsilon}^{DRED}$
F_2	$-\frac{1}{9}$	$\frac{71}{54}$	$\frac{59}{54}$	$\frac{25}{27}$	$-\frac{2}{9}$	$-\frac{10}{27}$	$-\frac{22}{27}$	$-\frac{10}{27}$	—	—	$-\frac{7}{9}$
F_3	$\frac{1}{9}$	$\frac{91}{54}$	$\frac{103}{54}$	$\frac{29}{27}$	$\frac{2}{9}$	$\frac{10}{27}$	$\frac{22}{27}$	$\frac{10}{27}$	—	—	$-\frac{11}{9}$
F_4	$\frac{1}{9}$	$\frac{25}{54}$	$\frac{37}{54}$	$\frac{19}{54}$	$\frac{2}{9}$	$\frac{10}{27}$	$\frac{22}{27}$	$\frac{10}{27}$	—	—	$-\frac{2}{9}$
F_4^{bg}	$\frac{1}{9}$	$\frac{25}{54}$	$\frac{37}{54}$	$\frac{19}{54}$	$\frac{2}{9}$	$\frac{10}{27}$	$\frac{22}{27}$	$\frac{10}{27}$	—	—	$-\frac{2}{9}$
F_7	—	$-\frac{2}{9}$	$-\frac{8}{9}$	$\frac{1}{9}$	—	—	$-\frac{4}{3}$	—	—	—	$\frac{2}{3}$

Table 9: The same as tab. (3) for the F diagrams with a $\gamma_L^\mu \otimes \gamma_{\mu R}$ vertex insertion.

	$\overline{D}$			
T_N	$\frac{1}{\epsilon^2}$	$\frac{1}{\epsilon}^{HV}$	$\frac{1}{\epsilon}^{NDR}$	$\frac{1}{\epsilon}^{DRED}$
F_2	$\frac{1}{9}$	$\frac{91}{54}$	$\frac{103}{54}$	$\frac{91}{54}$
F_3	$-\frac{1}{9}$	$\frac{71}{54}$	$\frac{59}{54}$	$\frac{71}{54}$
F_4	$-\frac{1}{9}$	$\frac{5}{54}$	$-\frac{7}{54}$	$\frac{5}{54}$
F_4^{bg}	$-\frac{1}{9}$	$\frac{5}{54}$	$-\frac{7}{54}$	$\frac{5}{54}$
F_7	—	$-\frac{2}{9}$	$\frac{4}{9}$	$-\frac{2}{9}$

Table 10: The same as tab. (4) for the F diagrams with a $\gamma_L^\mu \otimes \gamma_{\mu R}$ vertex insertion.

6 Anomalous Dimension Matrices

The anomalous dimension matrix appearing in eq. (3) is defined as

$$\hat{\gamma} = \frac{\alpha_s}{4\pi}\left(\hat{\gamma}_O + \frac{1}{2}(\gamma_f \hat{n}_f + \gamma_g \hat{n}_g) - \gamma_{m_b}\hat{S}_1 - \beta_0 \hat{S}_2\right), \tag{37}$$

where the diagonal matrices $\hat{n}_f$ and $\hat{n}_g$ respectively count the number of fermion and gluon external fields of the operator they are applied to, $(\hat{S}_1)_{ij} = \delta_{i7}\delta_{7j} + \delta_{i8}\delta_{8j}$, and $(\hat{S}_2)_{ij} = \delta_{i8}\delta_{8j}$. The anomalous dimensions due to the external fields and to the explicit couplings and masses are known to be

$$\begin{aligned} \gamma_f &= 2\frac{N^2-1}{2N} \quad , \quad \gamma_{m_b} = -6\frac{N^2-1}{2N} \\ \gamma_g &= -2\left(\frac{11}{3}N - \frac{2}{3}n_f\right) \quad , \quad \gamma_g^{bg} = -2\left(\frac{5}{3}N - \frac{2}{3}n_f\right) \\ \beta(\alpha_s) &= \frac{\alpha_s^2}{4\pi}\beta_0 + \ldots \;=\; -\frac{\alpha_s^2}{4\pi}\left(\frac{11}{3}N - \frac{2}{3}n_f\right) + \ldots \end{aligned} \tag{38}$$

The two values of γ_g refer to the Feynman and background gauge calculations.

The operator anomalous dimension $\hat{\gamma}_O$ is defined in terms of the matrix of the renormalization constants as shown in eq. (15). In turn this matrix has an expansion, in terms of the renormalized coupling constant α_s and the regularization parameter $\frac{1}{\epsilon}$, more involved than in other cases. In fact now the renormalization constants include an explicit dependence on the subtraction scale μ, starting already at order $O(\alpha_s^0)$, due to a mismatch in the dimension between 4-fermion and magnetic operators. Thus the usual expression of the anomalous dimension becomes

$$\hat{\gamma}_O = 2\hat{Z}^{-1}\left[(-\epsilon\alpha_s + \beta(\alpha_s))\frac{\partial}{\partial\alpha_s} + \mu^2\frac{\partial}{\partial\mu^2}\right]\hat{Z}, \tag{39}$$

while the multiple expansion of the matrix $\hat{Z}$ is given by

$$\begin{aligned} \hat{Z} \;=\; & 1 + \mu^{-2\epsilon}\left(\hat{Z}_0^{0,1} + \hat{Z}_1^{0,1}\frac{1}{\epsilon}\right) + \frac{\alpha_s}{4\pi}\left[\left(\hat{Z}_0^{1,1} + \hat{Z}_1^{1,1}\frac{1}{\epsilon}\right)\right. \\ & \left. + \mu^{-2\epsilon}\left(\hat{Z}_1^{1,2}\frac{1}{\epsilon} + \hat{Z}_2^{1,2}\frac{1}{\epsilon^2}\right)\right] + \ldots \end{aligned} \tag{40}$$

The coefficients are labeled as $\hat{Z}_c^{a,b}$, where a is the order in α_s, b is the number of loops involved in the calculation and c is the order in the $\frac{1}{\epsilon}$ expansion.

Using eqs. (39) and (40), we obtain

$$\begin{aligned} \hat{Z}_2^{1,2} &= 0 \\ \hat{\gamma}_O &= -2\hat{Z}_1^{1,1} - 4\left(\hat{Z}_1^{1,2} - \frac{1}{2}\hat{Z}_1^{1,1}\hat{Z}_0^{0,1} - \frac{1}{2}\hat{Z}_1^{0,1}\hat{Z}_0^{1,1}\right) \end{aligned} \tag{41}$$

In order to have a finite $\hat{\gamma}_O$ when D tends to 4 dimensions, the first of eqs. (41) must be satisfied. Then the second equation gives the anomalous dimension matrix in terms of the single pole coefficients and finite parts of the one and two loop diagrams, see also eq. (33). This equation is obtained by using the relations

$$\begin{aligned} \left(\hat{Z}_0^{0,1}\right)_{PP} &= \left(\hat{Z}_0^{1,1}\right)_{PP} = \left(\hat{Z}_1^{0,1}\right)_{PP} = 0 \\ \left(\hat{Z}_0^{0,1}\right)_{PE} &= \left(\hat{Z}_0^{1,1}\right)_{PE} = 0 \\ \left(\hat{Z}_1^{0,1}\right)_{EP} &= \left(\hat{Z}_1^{1,1}\right)_{EP} = \left(\hat{Z}_1^{1,2}\right)_{EP} = 0 \\ \hat{Z}_i^{0,1}\hat{Z}_j^{1,2} &= \hat{Z}_j^{1,2}\hat{Z}_i^{0,1} = 0, \qquad i,j = 0,1 \end{aligned} \tag{42}$$

which hold for our $\overline{MS}$ renormalization constants. P indices get values in the set of "physical", i.e. 4-dimensional, operators, while E refers to the "effervescent" ones. Moreover only matrix elements between "physical" operators are retained, the "effervescent" contribution being included in the last two terms of $\hat{\gamma}_O$ in eqs. (41). In fact the summed indices in the products of the $\hat{Z}$ matrices run over the full D-dimensional basis, including the "effervescent" operators.

The expression of $\hat{\gamma}_O$ in eq. (41) is similar to the next-to-leading order formula, see e.g. refs. [15, 20], even if this is a leading order calculation. In particular the third term in eq. (41) accounts for the well-known "effervescent" contribution coming from one loop 4-fermion diagrams. The fourth term includes the peculiar operators, present only in the DRED scheme, which are generated in $4-D$ dimensions by the diagrams in fig. (3). Both these terms are actually purely "effervescent", since they involve finite parts, which are not included in the $\overline{MS}$ renormalization constants as far as matrix elements between 4-dimensional operators are concerned. On the contrary, matrix elements connecting "physical" and "effervescent" operators must be retained in the matrix of the renormalization constants, even in the $\overline{MS}$ case.

In the last part of this section we summarize the results for the anomalous dimension matrices in the three considered schemes. The new calculation in the DRED scheme gives a matrix which is identical to the HV one. Hence the results reported here can also be found in ref. [7].

Splitting the anomalous dimension matrix as in eq. (5), we give the results for $\hat{\gamma}_r$, $\vec{\beta}_7$, $\vec{\beta}_8$ and γ_{77}, γ_{87}, γ_{88}.

The regularization scheme independent matrix $\hat{\gamma}_r$ is given by

$$\hat{\gamma}_r = \begin{pmatrix} -\frac{6}{N} & 6 & 0 & 0 & 0 & 0 \\ 6 & -\frac{6}{N} & -\frac{2}{3N} & \frac{2}{3} & -\frac{2}{3N} & \frac{2}{3} \\ 0 & 0 & -\frac{22}{3N} & \frac{22}{3} & -\frac{4}{3N} & \frac{4}{3} \\ 0 & 0 & 6-\frac{2n_f}{3N} & -\frac{6}{N}+\frac{2n_f}{3} & -\frac{2n_f}{3N} & \frac{2n_f}{3} \\ 0 & 0 & 0 & 0 & \frac{6}{N} & -6 \\ 0 & 0 & -\frac{2n_f}{3N} & \frac{2n_f}{3} & -\frac{2n_f}{3N} & -12\frac{N^2-1}{2N}+\frac{2n_f}{3} \end{pmatrix} \tag{43}$$

where N is the number of colours and $n_f = n_u + n_d$ is the number of active flavors.

The mixing of the magnetic operators Q_7 and Q_8 among themselves is also scheme independent and is given by

$$\begin{aligned} \gamma_{77} &= 8\frac{N^2-1}{2N} \\ \gamma_{87} &= 8\frac{N^2-1}{2N} \\ \gamma_{88} &= 4N - \frac{8}{N}. \end{aligned} \tag{44}$$

For the vectors $\vec{\beta}$, which depend on the regularization scheme, we obtain in HV and DRED

$$
\begin{aligned}
\vec{\beta}_7^{HV,DRED} &= \begin{pmatrix} 0 \\ \frac{8}{9}\frac{N^2-1}{2N} + \frac{12Q_u}{Q_d}\frac{N^2-1}{2N} \\ \frac{232}{9}\frac{N^2-1}{2N} \\ \frac{8n_f}{9}\frac{N^2-1}{2N} + \frac{12\bar{n}_f(N^2-1)}{2N} \\ -16\frac{N^2-1}{2N} \\ \frac{8n_f}{9}\frac{N^2-1}{2N} - \frac{12\bar{n}_f(N^2-1)}{2N} \end{pmatrix} \\
\vec{\beta}_8^{HV,DRED} &= \begin{pmatrix} 6 \\ \frac{22N}{9} - \frac{58}{9N} \\ \frac{44N}{9} - \frac{116}{9N} + 6n_f \\ 12 + \frac{22Nn_f}{9} - \frac{58n_f}{9N} \\ -4N + \frac{8}{N} - 6n_f \\ -8 - \frac{32Nn_f}{9} + \frac{50n_f}{9N} \end{pmatrix},
\end{aligned}
\tag{45}
$$

where $\bar{n}_f = n_d + \frac{Q_u}{Q_d} n_u$. The NDR result is given by

$$\vec{\beta}_7^{NDR} = \begin{pmatrix} 0 \\ \frac{-16}{9}\frac{N^2-1}{2N} + \frac{12Q_u}{Q_d}\frac{N^2-1}{2N} \\ \frac{184}{9}\frac{N^2-1}{2N} \\ -\frac{16n_f}{9}\frac{N^2-1}{2N} + \frac{12\bar{n}_f(N^2-1)}{2N} \\ 40\frac{N^2-1}{2N} \\ -\frac{16n_f}{9}\frac{N^2-1}{2N} - \frac{12\bar{n}_f(N^2-1)}{2N} + \frac{40N(N^2-1)}{2N} \end{pmatrix}$$

$$\vec{\beta}_8^{NDR} = \begin{pmatrix} 6 \\ \frac{22N}{9} - \frac{46}{9N} \\ \frac{44N}{9} - \frac{92}{9N} + 6n_f \\ 12 + \frac{22Nn_f}{9} - \frac{46n_f}{9N} \\ 4N - \frac{20}{N} - 6n_f \\ -8 - \frac{32Nn_f}{9} + \frac{62n_f}{9N} \end{pmatrix}. \tag{46}$$

7 Status of the Calculation of the QCD Correction to the $b \to s\,\gamma$ Decay

Let us start with the original calculations, from ref. [1] to ref. [3]. These works used the "reduced" basis. As we have shown, this approximation leads to scheme dependent results. Apart from this, there is no computational error in both the NDR and DRED calculations. However refs. [1, 3] did not include the contribution coming from the $O(\alpha_s^0)$ mixing among Q_5, Q_6 and the magnetic operators, which is present in NDR, while it vanishes in DRED. On the other hand the authors of ref. [2] overlooked the contributions of the "effervescent" counter-terms. Thus the two original NDR and DRED calculations obtained different final results. This difference led the authors of ref. [9] to the incorrect conclusion that the DRED scheme fails in this case. Now we know that those results can differ (and indeed they do) without implying any failure of the regularization scheme. A second, more specific, argument in ref. [9] was based on the explicit calculation of the sum of the diagrams $P2+P3$ in fig. (4). They computed this sum in DRED and in a 4-dimensional regularization scheme and obtained again different results. Incidentally eqs. (36) show that the sum $P2+P3$ is indeed scheme independent. We have checked that the two results of ref. [9] actually coincide, once one includes the contribution of the DRED "effervescent" counter-terms.

Coming to more recent calculations, the full basis and the already mentioned $O(\alpha_s^0)$ mixing have been taken into account, starting from ref. [4], so that now problems with the scheme independence of the Effective Hamiltonian are no more present, as shown in ref. [7]. However the three latest works on the subject [5, 6, 7] give three different results for some anomalous dimension matrix elements. In particular, using our normalization,

- ref. [5] gives $\gamma_{57} = -32$, $\gamma_{67} = \frac{4432}{27}$, $\gamma_{58} = 10$, $\gamma_{68} = -\frac{2210}{27}$;
- ref. [6] gives $\gamma_{57} = \frac{416}{3}$, $\gamma_{67} = \frac{7888}{27}$, $\gamma_{58} = -\frac{106}{3}$, $\gamma_{68} = -\frac{914}{27}$;
- ref. [7] gives $\gamma_{57} = \frac{160}{3}$, $\gamma_{67} = \frac{4432}{27}$, $\gamma_{58} = -\frac{74}{3}$, $\gamma_{68} = -\frac{1346}{27}$;

when $N = 3$ and $n_f = 5$. The origins of these differences have been clearly summarized in ref. [11]. We shortly repeat them here, taking our calculation as a reference

- the calculation of ref. [5] differs from our one because of the values of the diagrams $P2$ and $P3$ in tab. (8);
- the calculation of ref. [6] differs from our one because the results presented there do not include the "effervescent" counter-terms, as also stated in ref. [12].

Of course refs. [5] and [6] differ one from the other for both the two reasons listed above.

In our opinion, the results of ref. [6] actually agree with our ones. In fact we cannot see any reason not to include the "effervescent" counter-terms, which are known to be needed since a long time[4], see also eq. (41). Concerning ref. [5], we can just say that our diagrams, including those ones responsible for the difference, verify all the checks we have done, including those enforced by the scheme independence of the Effective Hamiltonian, eqs. (36). Up to now we have not been able to find any error in the calculations of $P2$ and $P3$ with a m_b mass insertion into the loop, which are actually quite easy to evaluate. Thus we are confident that our results are correct.

Anyway these differences still present in the literature are known to have a very little impact on the phenomenology of the radiative B decays. We plan to present our phenomenological analysis in a forthcoming paper [27].

Acknowledgments

We are grateful to G. Martinelli for his precious support in terms of suggestions and discussions. We acknowledge the partial support of the MURST, Italy, and INFN.

References

[1] B. Grinstein, R. Springer, M.B. Wise, Phys. Lett. B202 (1988) 138; Nucl. Phys. B339 (1990) 269.

[2] R. Grigjanis, P.J. O'Donnel, M. Sutherland and H. Navelet, Phys. Lett. B213 (1988) 355.

[3] G. Cella, G. Curci, G. Ricciardi and A. Viceré, Phys. Lett. B248 (1990) 181.

[4] Incidentally the final result is not scheme independent without the "effervescent" counter-terms.

[4] M. Misiak, Phys. Lett. B269 (1991) 161.

[5] M. Misiak, Nucl. Phys. B393 (1993) 23.

[6] K. Adel and Y.P. Yao, UM-TH-92/32 (1992).

[7] M. Ciuchini, E. Franco, G. Martinelli, L. Reina and L. Silvestrini, Phys. Lett. B316 (1993) 127.

[8] W. Siegel, Phys. Lett. B84 (1979) 193.

[9] R. Grigjanis, P.J. O'Donnel, M. Sutherland and H. Navelet, Phys. Lett. B237 (1990) 252.

[10] G. 't Hooft and M. Veltman, Nucl. Phys. B44 (1972) 189.

[11] M. Misiak, TUM-T31-46/93 (1993).

[12] K. Adel and Y.P. Yao, UM-TH 93-20, IP-ASTP-29-93 (1993).

[13] N. Cabibbo, Phys. Rev. Lett. 10 (1963) 1802.

[14] J. Kobayashi and M. Maskawa, Prog. Theor. Phys. 49 (1973) 652.

[15] M. Ciuchini, E. Franco, G. Martinelli and L. Reina, LPTENS 93/11, ROME prep. 92/913 and ULB-TH 93/03 (1993), to appear in Nucl. Phys. B.

[16] H. Simma, DESY 93-083 (1993).

[17] N.G. Deshpande and M. Nazerimonfared, Nucl. Phys. B213 (1983) 390.

[18] M.A. Shifman, A.I. Vainshtein and V.I. Zakharov, Phys. Rev. 18 (1978) 2583.

[19] A.J. Buras, M. Jamin, M.E. Lautenbacher and P.H. Weisz, Nucl. Phys. B370 (1992) 69.

[20] A.J. Buras and P.H. Weisz, Nucl. Phys. B333 (1990) 66.

[21] G. Altarelli, G. Curci, G. Martinelli, S. Petrarca, Nucl. Phys. B187 (1981) 461.

[22] M. Veltman, Schoonschip manual (1991), unpublished.

[23] D. Maison, Phys. Lett. B150 (1985) 39.

[24] H. Nicolai and P.K. Townsend, Phys. Lett. B93 (1980) 111.

[25] F.J. Gilman and M. Wise, Phys. Rev. D27 (1983) 1128.

[26] L.F. Abbott, Nucl. Phys. B185 (1981) 189.

[27] M. Ciuchini, E. Franco, G. Martinelli, L. Reina and L. Silvestrini, in preparation.